

2016

High Glucose Induces Reactivation of Latent Kaposi's Sarcoma-Associated Herpesvirus

Fengchun Ye

Case Western Reserve University, fxy63@case.edu

Yan Zeng

University of Nebraska-Lincoln

Jingfeng Sha

Case Western Reserve University

Tiffany Jones


University of Texas Health Sciences Center at San Antonio

Kurt Kuhne

University of Texas Health Sciences Center at San Antonio

See next page for additional authors

Follow this and additional works at: <https://digitalcommons.unl.edu/virologypub>

 Part of the [Biological Phenomena, Cell Phenomena, and Immunity Commons](#), [Cell and Developmental Biology Commons](#), [Genetics and Genomics Commons](#), [Infectious Disease Commons](#), [Medical Immunology Commons](#), [Medical Pathology Commons](#), and the [Virology Commons](#)

Ye, Fengchun; Zeng, Yan; Sha, Jingfeng; Jones, Tiffany; Kuhne, Kurt; Wood, Charles; and Gao, Shou-Jiang, "High Glucose Induces Reactivation of Latent Kaposi's Sarcoma-Associated Herpesvirus" (2016). *Virology Papers*. 312.
<https://digitalcommons.unl.edu/virologypub/312>

This Article is brought to you for free and open access by the Virology, Nebraska Center for at DigitalCommons@University of Nebraska - Lincoln. It has been accepted for inclusion in Virology Papers by an authorized administrator of DigitalCommons@University of Nebraska - Lincoln.

Authors

Fengchun Ye, Yan Zeng, Jingfeng Sha, Tiffany Jones, Kurt Kuhne, Charles Wood, and Shou-Jiang Gao

1 **High Glucose Induces Reactivation of Latent Kaposi's Sarcoma-**
2 **Associated Herpesvirus**

3
4 Fengchun Ye^{1,2,*}, Yan Zeng^{3,5}, Jingfeng Sha¹, Tiffany Jones², Kurt Kuhne², Charles
5 Wood³, and Shou-Jiang Gao^{2,4,*}

6
7 ¹Department of Biological Sciences, School of Dental Medicine, Case Western Reserve
8 University, 10900 Euclid Avenue, Cleveland, Ohio 44106. USA;

9 ²Department of Pediatrics, Greehey Children's Cancer Research Institute, University of
10 Texas Health Sciences Center at San Antonio, 7703 Floyd Curl Drive, San Antonio,
11 Texas 78229, USA;

12 ³Nebraska Center for Virology and School of Biological Sciences, University of
13 Nebraska, Lincoln, Nebraska 68583, USA;

14 ⁴Department of Molecular Microbiology and Immunology, Keck School of Medicine,
15 University of Southern California, California 90033, USA;

16 ⁵Current address: Department of Biochemistry and Key Laboratory of Xinjiang Endemic
17 and Ethic Diseases, Shihezi University School of Medicine, Xinjiang 83202, China.

18

19 ***Correspondence to:** Fengchun Ye, e-mail: fxxy63@case.edu; Shou-Jiang Gao, email:
20 shoujiag@usc.edu.

21

22 **Key words:** Diabetes, Kaposi's sarcoma, Blood glucose, Hydrogen peroxide, and KSHV

23 **ABSTRACT**

24 High prevalence of Kaposi's sarcoma (KS) is seen in diabetic patients. It is
25 unknown if the physiological condition of diabetes contributes to KS development. We
26 found elevated levels of viral lytic gene expression when Kaposi's sarcoma-associated
27 herpesvirus (KSHV) infected cells were cultured in high glucose medium. To
28 demonstrate the association between high glucose and KSHV replication, we xeno-
29 grafted telomerase-immortalized human umbilical vein endothelial cells that are infected
30 with KSHV (TIVE-KSHV) into hyperglycemic and normal nude mice. The injected cells
31 expressed significantly higher levels of KSHV lytic genes in hyperglycemic mice than in
32 normal mice. We further demonstrated that high glucose induced production of hydrogen
33 peroxide (H₂O₂), which down regulated silent information regulator 1 (SIRT1), a class-III
34 histone deacetylase (HDAC), resulting in epigenetic transactivation of KSHV lytic genes.
35 These results suggest that high blood glucose in diabetic patients contributes to
36 development of KS by promoting KSHV lytic replication and infection.

37

38 **AUTHORS' SUMMARY**

39 Multiple epidemiological studies have reported a higher prevalence of classic KS
40 in diabetic patients. By using both *in vitro* and *in vivo* models, we demonstrated an
41 association between high glucose and KSHV lytic replication. High glucose induces
42 oxidative stress and production of H₂O₂, which mediates reactivation of latent KSHV
43 through multiple mechanisms. Our results provide the first experimental evidence and
44 mechanistic support for the association of classic KS with diabetes.

45

46 **INTRODUCTION**

47 Kaposi sarcoma (KS) is a vascular neoplasia etiologically associated with
48 Kaposi's sarcoma-associated herpesvirus (KSHV) infection (1). KSHV establishes a life-
49 long persistent latent infection following acute infection. Reactivation of the latent virus
50 into productive lytic replication plays a pivotal role in the initiation and progression of
51 KS as viral load positively correlates with KS progression. Indeed, treatment of KS
52 patients with anti-herpesviral drugs effectively leads to regression of KS tumors (2-6).

53 Unlike iatrogenic or AIDS-associated KS, classic KS predominantly occurs in
54 elderly men of Mediterranean or Jewish decent, with no apparent immune suppression
55 (7). The exact cause for the development of classic KS remains undefined. Asthma,
56 allergies in males, topical corticosteroid use, and infrequent bathing have been suggested
57 as risk factors for classic KS (8-9). Multiple studies have also documented a high
58 prevalence of classic KS in patients with diabetes mellitus (10-13), a metabolic syndrome
59 that manifests with elevated levels of blood glucose and episodic ketoacidosis, either due
60 to a lack of insulin (Type-1 diabetes) or cellular resistance to insulin (Type-2 diabetes).
61 High levels of KSHV DNA and sero-positivity have been seen in diabetic patients (14-
62 16). However, no study has ever determined if diabetes is the cause or effect of KS and
63 whether high glucose level plays a role in the development of KS.

64 In the present study, we found increased levels of viral lytic gene expression when
65 KSHV-infected primary effusion lymphoma cells were cultured in medium containing
66 high levels of glucose. To further examine the association between high blood glucose
67 and KSHV replication, we generated hyperglycemic nude mice with streptozotocin
68 (STZ), which damages pancreatic β cells to result in hypoinsulinemia and hyperglycemia

69 (17). We then xeno-grafted telomerase-immortalized human umbilical vein endothelial
70 cells (18) that are re-infected with a recombinant Kaposi's sarcoma-associated
71 herpesvirus [TIVE-KSHV (BAC16)] (19), into the hyperglycemic and control healthy
72 nude mice. The original TIVE-KSHV cells were malignantly transformed and grow
73 "KS-like" tumors in nude mice (18). Although hyperglycemia did not seem to enhance
74 tumor growth, the injected TIVE-KSHV (BAC16) cells expressed significantly higher
75 levels of KSHV lytic genes in hyperglycemic mice than in normal mice. Results from
76 cells cultured *in vitro* demonstrate that high glucose induces production of H₂O₂, which
77 has been previously shown to trigger reactivation of latent KSHV through activation of
78 the MAPK pathways (20-21). Interestingly, H₂O₂ also mediates down regulation of the
79 class-III HDAC SIRT1 (22) to induce histone hyperacetylation of viral chromatin,
80 resulting in active transcription of KSHV lytic genes. Our results suggest that H₂O₂
81 mediates high glucose induction of KSHV lytic gene expression and replication through
82 multiple mechanisms.

83 To our knowledge, this study provides the first experimental evidence to support
84 an association of diabetes with development of KS that has been suggested by previous
85 epidemiological studies.

86

87 **MATERIALS and METHODS**

88 **Cell culture, media, and reagents**

89 TIVE-KSHV cells, originally infected with native KSHV (18), were cultured in
90 Dulbecco's Modified Eagle Medium (DMEM) medium plus 10% fetal bovine serum
91 (FBS). We re-infected these cells with the recombinant KSHV BAC16 to obtain TIVE-

92 KSHV (BAC16) cells that stably express green fluorescence protein (GFP). RPMI 1640
93 medium without glucose was purchased from ThermoFisher Scientific (Waltham,
94 Massachusetts, USA). BCBL1 cells were grown in RPMI 1640 medium with 1, 3, or 6
95 g/L D-glucose plus 10% FBS. Primary human umbilical vein endothelial cells
96 (HUVECs) were grown in EBM-2 medium with growth factor supplements (Lonza,
97 Allendale, New Jersey, USA).

98 A mouse monoclonal antibody to KSHV lytic protein RTA was a gift from the
99 Pasteur Research Institute in Shanghai, China. A mouse monoclonal antibody to KSHV
100 lytic protein K8 α was purchased from MyBiosource, Inc. (San Diego, California, USA).
101 A rat antibody to KSHV latent nuclear antigen (LANA) was purchased from Advanced
102 Biotechnologies, Inc. (Columbia, Maryland, USA). A mouse monoclonal antibody to
103 SIRT1 was purchased from EMD Millipore (Temecula, California, USA). D-glucose and
104 L-glucose were purchased from Sigma-Aldrich.

105

106 **Generation of hyperglycemic mice and xeno-grafting of TIVE-KSHV (BAC16) cells**

107 A total number of 32 athymic nude mice (4 week old, female) were purchased
108 from Jackson Laboratory (Bar Harbor, ME, USA). The blood glucose level of each
109 mouse was measured before any treatment by using a glucose meter. The mice were then
110 randomly separated into two groups, one being treated with intra-peritoneal (IP) injection
111 of Streptozotocin (STZ, Sigma-Aldrich) at a dose of 200 mg/kg body mass, twice a week
112 for 2 weeks. The other group of untreated mice was used as a control. Two weeks after
113 the last STZ treatment, the blood glucose level of each mouse from both groups was
114 measured again to confirm development of hyperglycemia in the treated mice. Equal

115 numbers of TIVE-KSHV (BAC16) cells at 5×10^6 cells per injection site, 2 sites per
116 mouse, were then subcutaneously injected into each mouse at the abdominal region.
117 Tumor volumes (length x width x height) were measured once a week with a caliper. At
118 the end of experiments, all tumors were surgically removed from the mice. All
119 procedures were carried out in strict accordance with the recommendations in the Guide
120 for the Care and Use of Laboratory Animals of the National Institutes of Health and
121 following a protocol (2011-0802) that was approved by the Institutional Animal Care and
122 Use Committee (IACUC) at Case Western Reserve University.

123

124 **Immuno-chemical staining and imaging**

125 Fresh frozen sections were prepared from the surgically removed tumors. A
126 standard procedure for preparation and staining of acetone-fixed frozen tissue sections
127 was followed, using primary antibodies to KSHV small capsid protein (ORF65), latent
128 protein LANA, and control IgG. After multiples washes with PBS, the primary antibody-
129 antigen signals were revealed with a biotinylated secondary antibody and streptavidin-
130 horseradish peroxidase, and DAB (3,3'-diaminobenzidine) detection system (Biolegend,
131 San Diego, California, USA). DAPI was used for nuclear staining. Images were captured
132 under a microscope (Carl Zeiss, Inc., Thornwood, NY).

133

134 **Isolation of Total RNAs and Quantification of mRNA by qRT-PCR**

135 Total RNAs were isolated using a RNA purification kit from QIAGEN, which
136 includes a step to remove residual genomic DNA prior to RNA purification. Reverse
137 transcription (RT) of total RNA was performed by using Superscript Transcriptase II

138 (Invitrogen, Carlsbad, CA). qRT-PCR was conducted to quantify different viral
139 transcripts using primers described previously (23). The mRNA level of the
140 housekeeping gene β -actin was used as a reference for normalization, using the primers
141 5'ATTGCCGACAGGATGCAGA3' (forward) and
142 5'GAGTACTTGCGCTCAGGAGGA3'(reverse). All qRT-PCR reactions were carried
143 out in triplicates.

144

145 **KSHV Virion Production and Titration**

146 The culture supernatants of BCBL1-BAC36 cells were collected 5 days after
147 culturing in RPMI 1640 medium plus 10% FBS and various concentrations of D-glucose,
148 followed by low-speed centrifugation (4,000 g, 15 min) to remove cellular debris. To
149 determine the relative viral titers in the supernatants, 1 ml of the supernatant was used to
150 infect HUVECs in 6-well plates. At 72 h post-infection, cells were harvested and
151 counted with a hemocytometer under a fluorescent microscope. The numbers of KSHV
152 infected GFP-positive cells and the numbers of total cells from 8 independent readings
153 were used to calculate the average percentage of GFP-positive cells, which was used as
154 the relative viral titer of the supernatant in question.

155

156 **Chromatin Immuno-Precipitation (ChIP) Assay**

157 Equal numbers of BCBL1-BAC36 cells (8×10^6 cells) were cultured in RPMI
158 1640 medium with various concentrations of D-glucose with and without catalase (400
159 unites/ml) for 24 h, followed by fixation with 0.5% formaldehyde for 15 min. Chromatin
160 suspensions were prepared, and ChIP assays were performed using a ChIP assay kit

161 (Invitrogen) with antibodies to RNA polymerase II (RN Pol II), acetylated histone-4
162 (H4K12-Ac), histone-3 (H3K9-Ac), histone-3 (H3), LANA, and rabbit IgG, all from
163 Millipore, as well as a rat monoclonal antibody to LANA and a rat IgG (as control) as
164 described above. DNA from input and the end ChIP products were isolated by using a
165 DNA purification kit (QIAGEN). The purified DNA was re-suspended in 200 μ l sterile
166 water, and used for qPCR quantification for specific viral chromatin with the following
167 primers: 5'CTCATCGTCGGAGCTGTCACACG3' (RTA promoter-forward) and
168 5'TCTCCCGATGGCGACGTGCACTAC3' (RTA promoter-reverse) from RTA
169 (ORF50) promoter region.

170

171 **Measurement of intracellular H₂O₂**

172 BCBL1-BAC36 cells were cultured in RPMI 1640 medium plus 10% FBS with 1,
173 3, and 6 g/L D-glucose for 24 hours. The cells were collected and washed twice with ice-
174 cold PBS, and re-suspended in 1 x assay buffer of the OxiSelect™ hydrogen
175 peroxide/peroxidase assay kit from Cell Biolabs, Inc. (San Diego, California, USA) at a
176 concentration of 2 x 10⁶/ml. The cells were homogenized by sonication, followed by
177 high speed centrifugation (10,000 g, 15 minutes at 4°C). The supernatants and 1 x assay
178 buffer (as background) were loaded into 96-well plate for measurement of the relative
179 levels of H₂O₂, with 6 repeats per sample. In parallel, a series of different concentrations
180 (0 to 10 μ M) of H₂O₂ were loaded into the same plate. The fluorescence H₂O₂ detection
181 reaction was read under a fluorescence microplate reader (BIO-TEK, Winooski, Vermont,
182 USA) at 560 nm (excitation) and 600 nm (emission). Upon subtraction of each reading
183 with that of the background, a standard curve was established with relative fluorescence

184 units (RFU) from the different concentrations of H₂O₂, and the concentrations of H₂O₂ in the
185 samples were determined by comparing RFU of the samples with the standard curve.

186

187 RESULTS

188 Cells cultured in high concentrations of D-glucose display increased KSHV lytic 189 gene expression

190 To test the effect of high concentration of glucose on KSHV gene expression, we
191 conducted independent experiments in three different laboratories. The Wood laboratory
192 cultured the original KSHV-infected BCBL1 cells in RPMI 1640 medium containing 1,
193 3, and 6 g/L D-glucose, which are equivalent to 100, 300, and 600 mg/dL as measured by
194 clinic glucose meters, respectively. Clearly, BCBL1 cells expressed significantly higher
195 levels of RTA and K8.1 mRNA (Fig. 1A), as well as RTA and K8 α proteins when
196 cultured in medium containing 3 and 6 g/L D-glucose (Fig. 1B and C).

197 Adding more D-glucose also changes the osmolality of the medium. To rule out
198 possible effect of osmolality on KSHV gene expression, the Gao and Ye laboratories
199 cultured BCBL1 cells carrying the recombinant KSHV, BAC36 (24), in RPMI 1640
200 medium containing 1, 3, and 6 g/L of D-glucose and 5, 3, and 0 g/L L-glucose,
201 respectively. L-glucose, which cannot be metabolized by the cells, was used to balance
202 the osmolality in medium with lower levels of D-glucose, in order for all cells to be
203 compared with the same osmolality. As shown in Fig. 1E, F, and G, under these
204 conditions, higher concentrations of D-glucose increased expression of RTA and ORF65
205 in BCBL1-BAC36 cells. Similar effects were also seen in TIVE-KSHV (BAC16) cells
206 (Fig. 1D). In addition, BCBL1-BAC36 cells cultured in high levels of D-glucose

207 produced higher titers of virions (Fig. 1H). Collectively, these results indicate that high
208 glucose enhances KSHV lytic gene expression and replication in different types of cells.

209

210 **Generation of hyperglycemic nude mice and xeno-grafting of TIVE-KSHV cells**

211 To further examine the association between high blood glucose in diabetic KS
212 patients and KSHV replication, we next generated hyperglycemic nude mice by using the
213 commonly used antibiotic STZ. Before treatment, the blood glucose level of each mouse
214 was measured using a glucose meter. All 32 mice had a blood glucose level within the
215 normal range (100 to 140 mg/dL) (Fig. 2A). The mice were then randomly divided into
216 two groups. One group of mice were injected with STZ at a dose of 200 mg/kg body
217 mass, twice weekly for 2 weeks, and the second group were injected with a placebo
218 (PBS). Two weeks after the treatment, we measured the blood glucose levels of all mice
219 again. All STZ-treated mice displayed permanent diabetic levels of blood glucose (Fig.
220 2A) and symptoms of diabetes such as excessive thirst and loss of weight (Fig. 2B).

221 We then subcutaneously injected TIVE-KSHV (BAC16) cells at the abdominal
222 region at a dose of 5×10^6 cells per injection site, two sites per mouse, into the two
223 groups of mice for tumor development. Eight weeks after inoculation, we surgically
224 collected the tumors. As shown in Fig. 2C and D, no significant difference in tumor
225 volume was seen between the two groups, except two of the STZ-treated mice developed
226 a secondary tumor at the neck region. These secondary tumors had fewer cells that
227 expressed KSHV latent protein LANA and contained large numbers of mouse
228 inflammatory cells expressing the mouse macrophage marker F4/80 (data not shown).

229

230 **TIVE-KSHV (BAC16) cells express higher levels of KSHV lytic genes in**
231 **hyperglycemic mice**

232 To examine how blood glucose level impacts viral gene expression, we isolated
233 total RNA from 8 tumors from each group of mice and measured the mRNA levels of
234 KSHV replication and transcription activator (RTA, ORF50) by qRT-PCR. All tumors
235 from STZ-treated mice express higher levels of RTA mRNA (Fig. 3A). We then
236 extracted total proteins from 8 tumors of each group and conducted Western blot analysis
237 to measure viral proteins. As shown in Fig. 3B, all 8 tumors from STZ-treated mice
238 expressed much higher levels of RTA protein than the control mice. To further confirm
239 increased expression of KSHV lytic genes in tumors from STZ-treated mice, we
240 performed immune-histochemical staining on sections of the other 8 tumors from each
241 group with a monoclonal antibody to KSHV small capsid protein (ORF65). As shown in
242 Fig. 3C and D, the numbers of cells expressing ORF65 are 4.8 times higher in tumors
243 from STZ-treated mice than in tumors from the control mice.

244 Since we waited two weeks after the last STZ treatment before injecting TIVE-
245 KSHV (BAC16) cells into the mice, it is unlikely that the increased expression of RTA
246 and ORF65 resulted from STZ treatment itself. To rule out that possibility, we cultured
247 TIVE-KSHV (BAC16) cells in the absence or presence of STZ, followed by Western blot
248 detection of RTA and LANA proteins. As shown in Fig. 3E, STZ treatment had little
249 effect on expression of RTA and LANA. Hence, the elevated levels of blood glucose in
250 STZ-treated mice are responsible for the increased expression of KSHV lytic genes.

251

252 **High concentrations of glucose enhances KSHV lytic gene expression by inducing**
253 **H₂O₂**

254 Metabolic syndromes including diabetes are well known for the production of
255 excessive amounts of reactive oxygen species (ROS) such as H₂O₂ (25-30), which has
256 previously been shown to trigger reactivation of latent KSHV into lytic replication (20-
257 21, 31). To monitor changes in the level of intracellular H₂O₂, we used a previously
258 established BCBL1 cell line that stably expresses the H₂O₂ sensor protein Hyper-cyto
259 (21). The Hyper-cyto protein exhibits two excitation peaks at 420 and 500 nm and one
260 emission peak at 516 nm. Upon exposure to H₂O₂, the excitation peak at 420 nm
261 decreases in proportion to the increase in the peak at 500 nm, and cells become yellow
262 fluorescent when intracellular H₂O₂ surpasses the threshold level (32). We cultured these
263 cells in RPMI 1640 medium containing 1, 3, and 6 g/L D-glucose for 24 hours
264 respectively. As shown in Fig. 4A and B, the intracellular level of H₂O₂ increased
265 significantly when cells were cultured in higher concentrations of D-glucose. To further
266 confirm that high glucose induces H₂O₂ production, we cultured BCBL1-BAC36 cells in
267 RPMI 1640 medium containing 1, 3, and 6 g/L D-glucose for 24 hours respectively,
268 prepared cell lysates from equal numbers (2 x 10⁶) of cells in 1 ml assay buffer, and
269 measured their relative intracellular H₂O₂ concentrations by using a hydrogen
270 peroxide/peroxidase assay kit from Cell Biolabs, Inc. Cells cultured in medium containing 3
271 and 6 g/L D-glucose definitely produced higher levels of H₂O₂ (Fig. 4C).

272 To demonstrate that H₂O₂ was responsible for the increased KSHV lytic gene
273 expression, we next cultured BCBL1-BAC36 cells in RPMI 1640 medium containing 1
274 and 6 g/L D-glucose respectively, in the absence or presence of catalase or the

275 antioxidants N-acetyl-cysteine (NAC) and glutathione. As shown in Fig. 4D, catalase
276 abolished high glucose-induced transcription of RTA and ORF65. The three different
277 antioxidants inhibited high glucose-induced expression of ORF65 protein in a dose-
278 dependent manner (Fig. 4E). Collectively, these results suggest that induction of KSHV
279 lytic gene expression by high glucose is mediated by H₂O₂.

280

281 **High glucose down regulates class-III HDAC SIRT1 to increase histone acetylation**
282 **and transactivate viral chromatins**

283 We previously showed that H₂O₂ activated the MAP kinases ERK-1/2, JNK, and
284 p38 to induce expression of KSHV lytic genes (21). Consistent with our previous finding,
285 BCBL1-BAC36 cells cultured in medium containing high concentration of D-glucose
286 displayed increased phosphorylation of ERK1/2, JNK, and p38 and expression of KSHV
287 lytic protein RTA, which can be inhibited by catalase (Fig. 5A). In addition, inhibitors of
288 ERK1/2, JNK, and p38 significantly inhibited high glucose induction of RTA
289 transcription (Fig. 5B), thus confirming a critical role of MAPK activation in high
290 glucose induction of RTA expression.

291 To investigate other mechanisms that might be involved in high glucose induction
292 of KSHV lytic replication, we examined the expression of SIRT1, which is a member of
293 class-III HDAC and a key factor involved in the development of diabetes (33-39). In
294 addition, several studies have demonstrated the involvement of SIRT1 in the regulation
295 of KSHV lytic gene expression through epigenetic remodeling (40-42).

296 Immuno-fluorescence antibody (IFA) staining showed that SIRT1 expression was
297 substantially reduced in BCBL1-BAC36 cells cultured in medium containing 6 g/L D-

298 glucose compared to cells cultured in medium containing 1 g/L D-glucose (Fig. 6A and
299 B). Consistent with the IFA results, data from Western blot analysis showed that the
300 protein level of SIRT1 was reduced by D-glucose in a dose-dependent manner (Fig. 7A).
301 To examine if H₂O₂ plays a role in SIRT1 down regulation, we cultured BCBL1-BAC36
302 cells in medium containing low and high glucose in the presence of various doses of
303 catalase. As shown in Fig. 7B, catalase dose-dependently blocked SIRT1 down regulation
304 in cells that were cultured in medium containing 6 g/L D-glucose. In a parallel
305 experiment, we found that treating BCBL1-BAC36 cells with H₂O₂ also resulted in
306 SIRT1 down regulation, which could be blocked by catalase as well (Fig. 7C). Together,
307 these results suggest that H₂O₂ mediates SIRT1 down regulation in cells that are cultured
308 in medium containing high concentration of glucose.

309 As a consequence of SIRT1 down regulation, BCBL1-BAC36 cells cultured in
310 medium containing high concentrations of D-glucose displayed increased levels of
311 acetylated histones, which could be reduced by adding catalase to the culture medium
312 (Fig. 7D). To demonstrate that these epigenetic changes indeed occur in viral
313 chromatin, we next conducted ChIP assays. By performing qPCR using primers specific
314 for the promoter region of KSHV lytic gene RTA, we detected significantly higher levels
315 of acetylated histones and RNA polymerase II in this region of viral chromatin when cells
316 were cultured in medium containing high concentrations of glucose (Fig. 5E and F).
317 These results suggest that, in addition to activation of MAPK pathways, high glucose also
318 transactivate KSHV lytic gene expression via epigenetic modifications of the RTA
319 promoter region.

320

321 **DISCUSSION**

322 Multiple studies have reported high prevalence of classic KS in patients with
323 diabetes mellitus (10-13), and KSHV DNA was detected in more than 50% of type-2
324 diabetic patients (14-16). These clinical studies seem to suggest that diabetes patients are
325 more prone to KSHV infection and that diabetes is a risk factor for development of
326 classic KS. However, whether this metabolic syndrome really contributes to KS tumor
327 development has never been experimentally tested.

328 Type-1 diabetes results from insulin deficiency due to the lack of insulin-
329 producing β cells in the pancreas. In contrast, type-2 diabetes occurs in adults as a
330 consequence of the development of cellular resistance to insulin. Despite the different
331 mechanisms, a common outcome of both types of diabetes is high glucose levels in the
332 plasma. In the present study, we found increased levels of KSHV lytic gene expression
333 when KSHV infected BCBL1 and TIVE-KSHV cells were cultured in media containing
334 diabetic levels of glucose. In full support of data from the *in vitro* study, TIVE-KSHV
335 cells also displayed substantially higher expression of KSHV lytic genes in
336 hyperglycemic mice than in mice with normal level of blood glucose. These results
337 strongly suggest that high levels of blood glucose promote development of KS by
338 inducing productive KSHV lytic replication.

339 One of the manifestations by metabolic syndromes such as obesity and diabetes is
340 production of excessive levels of ROS (25-30). By using a previously established BCBL1
341 cell line that stably expressing the H_2O_2 sensor protein pHyper-cyto (21), we
342 demonstrated that cells cultured in high concentrations of glucose produce increased
343 levels of intracellular H_2O_2 . This result was further confirmed by another intracellular

344 H₂O₂ measurement assay. Notably, addition of catalase, which converts H₂O₂ into H₂O
345 and O₂, and the anti-oxidants NAC and glutathione, effectively blocked high glucose
346 induction of KSHV lytic gene expression in a dose-dependent manner. Therefore, H₂O₂
347 mediates high glucose induction of KSHV lytic gene expression, which further supports
348 previous reports that H₂O₂ is an important physiological factor involved in reactivation of
349 latent KSHV (20-21, 31). Interestingly, H₂O₂ has also been shown to enhance viral entry
350 (43-45). It is therefore highly possible that the hyperglycemic environment in diabetic KS
351 patients contributes to development of KS by promoting both productive KSHV
352 replication and recurrent *de novo* infection.

353 Similar to stimulation with H₂O₂ (21), culturing cells in medium containing high
354 concentrations of D-glucose also activates ERK1/2, JNK, and p38, and inhibitors of these
355 MAPK pathways inhibit high glucose induction of KSHV gene expression. Interestingly,
356 we found that high glucose and H₂O₂ also cause down regulation of the class-III HDAC
357 SIRT1, leading to increased levels of histone acetylation in the promoter region of KSHV
358 key lytic gene RTA. Thus, high glucose also engages this epigenetic mechanism to
359 promote KSHV lytic gene expression. SIRT1 is well known for its anti-aging, anti-
360 oxidative stress, and anti-inflammation properties (22, 46-47), and down regulation of
361 SIRT1 has been linked to development of diabetes (48). Suppression of SIRT1 has been
362 shown to trigger reactivation of latent KSHV (42, 49). SIRT1 is a member of the Sirtuin
363 protein family that couples histone lysine deacetylation to NAD hydrolysis (50-52). The
364 dependence of SIRT1 on NAD links its enzymatic activity directly to the energy status of
365 cells via the cellular NAD to NADH ratio, the absolute levels of NAD, NADH or
366 nicotinamide, or a combination of these variables.

367 The development of KS is a complex process. KSHV infection resulting from
368 productive lytic replication plays an essential role in the initiation and progression of KS.
369 However, in already formed KS tumors, KSHV-infected tumor cells are predominantly
370 latent (53). Inflammatory cytokines, stress, and ROS are known to stimulate KSHV
371 reactivation from latency (54). Under highly inflammatory and stressful conditions such
372 as diabetes, it is expected that the latent virus undergoes reactivation. In this study, we
373 xeno-grafted the KS tumor model cell line TIVE-KSHV (BAC16) into normal and
374 hyperglycemic nude mice. While no obvious difference in tumor growth was seen
375 between the two groups of mice, we did find significantly higher numbers of TIVE-
376 KSHV (BAC16) cells undergoing lytic replication in hyperglycemic mice than in normal
377 mice. Nevertheless, the majority of TIVE-KSHV cells in tumors from hyperglycemic
378 mice remain latently infected, suggesting that the virus might have evolved unique
379 mechanisms to overcome the highly inflammatory and stressful conditions to maintain
380 latency. One possible mechanism might be through modulation of the cellular metabolic
381 status. In support to this hypothesis, our recent study demonstrated that KSHV inhibits
382 cellular aerobic glycolysis and oxidative phosphorylation by inhibiting expression of
383 GLUT1 and GLUT3, thus preventing overflow of the metabolic pathways and
384 maintaining the homeostasis of the latently infected and malignantly transformed cells
385 (55).

386 In summary, our study provides the first evidence for a link between diabetes and
387 higher levels of KSHV replication, which may lead to development of classic KS. Our
388 results highlight H₂O₂ as the mediator for high glucose induction of KSHV lytic

389 replication through multiple mechanisms, which may shed lights on development of new
390 strategies to prevent KSHV infection and KS development in diabetic patients.

391

392 **ACKNOWLEDGEMENT**

393 The present work was supported by the Immunology Alliance Fund from Case Western
394 Reserve University to Fengchun Ye. This work was also supported by grants from NIH
395 to Shou-Jiang Gao (CA096512, CA124332, CA132637, DE025465 and CA197153); and
396 to Charles Wood (CA65903, P30 GM103509 and Fogarty D43 TW01492). We thank Dr.
397 Ke Lan from the Pasteur Research Institute in Shanghai, China for providing antibodies
398 to KSHV lytic protein RTA. We are grateful to Dr. Jae U. Jung from University of
399 Southern California, USA for providing the recombinant KSHV BAC16. We declare no
400 conflict of interest.

401

402

403 **FIGURE LEGENDS**

404 Figure-1. Cells cultured in medium containing higher concentrations of D-glucose
405 express increased levels of KSHV lytic genes. **A**, relative levels of RTA and K8.1
406 mRNAs in BCBL1 cells that were cultured in RPMI 1640 medium containing 1, 3, and 6
407 g/L D-glucose (D-Glu) for 24 hours respectively. **B**, Western blot detection of RTA and
408 K8 α proteins from BCBL1 cells treated as described in **A**. **C**, relative levels of RTA and
409 K8 α protein in Western blots shown in **B**. The intensity of RTA or K8 α band from each
410 sample was first normalized to that of the β -tubulin band from the same sample. The
411 levels of RTA and K8 α proteins in cells cultured in medium containing 1 g/L D-glucose

412 were then set as the reference with a value of 1.0, and the relative levels of these proteins
413 in other cells were the ratios between their band intensities and that of the reference. **D**,
414 relative levels of RTA and ORF57 mRNAs in TIVE-KSHV cells cultured in DMEM
415 medium containing 10% FBS and 1 or 6 g/L D-glucose (D-Glu) plus 5 or 0 g/L L-glucose
416 (L-Glu) respectively. **E**, relative levels of ORF50 (RTA) and ORF65 mRNAs in
417 BCBL1-BAC36 that were cultured in RPMI 1640 medium containing 10% FBS and 1, 3,
418 or 6 g/L D-glucose (D-Glu) plus 5, 3, or 0 g/L L-glucose (L-Glu) for 24 hours (for RTA
419 mRNA) and 72 hours (for ORF65 mRNA), respectively. **F**, Western blot detection of
420 RTA and ORF65 proteins from BCBL1-BAC36 cells treated as described in **E**; **G**,
421 relative levels of RTA and ORF65 proteins in Western blots shown in **F**, which were
422 calculated as described in **C**. **H**, percentages (%) of GFP-positive HUVECs at 48 hours
423 post infection (hpi) with supernatant from equal numbers (8×10^6) of BCBL1-BAC36
424 cells that were cultured in RPMI 1640 medium containing 10% FBS, 1, 3, or 6 g/L D-
425 glucose (D-Glu) plus 5, 3, or 0 g/L L-glucose (L-Glu) for 5 days respectively. All qRT-
426 PCR reactions consisted of triplicates, and the differences in relative mRNA levels (fold)
427 of RTA, ORF57, K8.1, and ORF65 between cells cultured in medium containing 1 g/L
428 D-glucose and those cultured in medium containing 3 or 6 g/L D-glucose were all
429 significant with P values < 0.005 .

430

431 Figure-2. Generation of hyperglycemic nude mice and xeno-grafting TIVE-KSHV
432 (BAC16) cells for tumor development. A total of 32 athymic nude mice (4 weeks old,
433 female) were randomly separated into two groups, with one group of mice being treated
434 with STZ (200 mg/kg body mass, 2 IP injections per week, for 2 weeks) to develop

435 hyperglycemia and the other group of mice injected with PBS (placebo) as a control.
436 Equal numbers (5×10^6 /injection site, 2 sites/mouse) of TIVE-KSHV (BAC16) cells were
437 subcutaneously injected into the mice for tumor development two weeks after the last
438 STZ treatment. **A**, average blood glucose levels of STZ-treated mice and un-treated mice
439 (control) measured at 4 and 12 weeks after the first STZ treatment. **B**, average weights of
440 the two groups of mice at 2 and 12 weeks after the first STZ treatment. **C**, representative
441 tumors from the two groups of mice collected at the end of experiment. **D**, average
442 volumes (length x width x height) of tumors from the two groups of mice at different
443 week post inoculation of TIVE-KSHV (BAC16) cells.

444

445 Figure-3. Tumors from hyperglycemic mice express significantly higher levels of KSHV
446 lytic gene expression. **A**, average mRNA levels of KSHV lytic gene ORF50 (RTA) from
447 8 tumors of STZ-treated and untreated (control) mice respectively. **B**, Western blot
448 detection of lytic protein RTA and latent protein LANA from 8 tumors of each group. β -
449 tubulin was used as loading control. **C**, immuno-chemical staining of KSHV small capsid
450 protein (ORF65) and LANA on tumors from three STZ-treated and three control mice
451 (M1, M2, and M3). Staining with mouse or rat IgG was done in parallel as a negative
452 control. **D**, average numbers of ORF65-positive cells per microscopic field in tumor
453 sections from the two groups of mice. **E**, Western blot detection of RTA and LANA
454 proteins from TIVE-KSHV (BAC16) cells that were cultured with and without STZ (1
455 μ M) and TPA (25 ng/ml) for 24 hours respectively.

456

457

458 Figure-4. High glucose induces H₂O₂ to induce KSHV lytic gene expression. **A** and **B**,
459 BCBL1 cells stably expressing the H₂O₂ sensor protein pHyper-cyto were used to
460 measure the relative levels of intracellular H₂O₂. The number of cpYFP-positive cells (**A**)
461 and fluorescence intensity (**B**) were quantified by flow cytometry analysis, following a 24
462 hours culture in RPMI 1640 medium containing 10% FBS and 1 (red), 3 (green), or 6
463 (purple) g/L D-glucose respectively. Regular BCBL1 cells cultured in RPMI 1640
464 medium containing 10% FBS and 2 g/L D-glucose were used as a background control for
465 flow cytometry analysis (black). Culture with each glucose concentration consisted of 6
466 replicates. **C**, relative intracellular H₂O₂ concentrations from equal numbers (2 x10⁶) of
467 BCBL1-BAC36 cells that were cultured as described in **A** and **B**. Measurement of H₂O₂
468 was carried out by using the OxiSelect™ hydrogen peroxide/peroxidase assay kit from Cell
469 Biolabs, Inc. **D**, ORF50 (RTA) and ORF65 mRNA levels in BCBL1-BAC36 cells
470 cultured in RPMI 1640 medium containing 1 or 6 g/L D-glucose (D-Glu) in the presence
471 or absence of 400 U/ml of catalase (Cat) for 24 h (for RTA mRNA) and 72 h (for ORF65
472 mRNA) respectively. Differences in mRNA levels between cells cultured in medium
473 containing 1 g/L and those cultured in medium containing 6/L D-glucose or between
474 culture with and without catalase were all significant with P values <0.005. **E**, Western
475 blot detection of KSHV small capsid protein (ORF65) in BCBL1-BAC36 cells cultured
476 in RPMI 1640 medium containing 1 or 6 g/L D-glucose (D-Glu) in the presence of
477 different doses of catalase and antioxidants NAC and glutathione for 72 hours
478 respectively.

479

480 Figure-5. High glucose activates MAPK pathways to induce KSHV gene expression. **A**,
481 Western blot detection of ERK-1/2, JNK, p38, and their phosphorylated counterparts, as
482 well as RTA and β -tubulin in BCBL1-BAC36 cells that were cultured in RPMI 1640
483 medium containing 1 or 6 g/L D-glucose (D-Glu), or stimulated with 400 μ M H₂O₂, in
484 the presence or absence of 200 U/ml catalase (Cat) for 24 hours. **B**, levels of RTA
485 mRNA in BCBL1-BAC36 cells that were cultured in RPMI 1640 medium with 1 or 6 g/L
486 D-glucose (D-Glu) in the presence or absence of the different MAPK inhibitors for 24
487 hours. Concentrations of the inhibitors were as described previously (21).

488

489 Figure-6. High glucose down regulates expression of class-3 HDAC SIRT1. **A**, IFA
490 staining of SIRT1 (red) in BCBL1-BAC36 cells cultured in RPMI 1640 medium
491 containing 10% FBS and 1 or 6 g/L D-glucose for 24 h, using a mouse monoclonal
492 antibody to SIRT1 and a rabbit anti-mouse IgG conjugated to Alexa Fluor®-594. DAPI
493 was used for nuclear staining. The cells were imaged and analyzed under a fluorescence
494 microscope with a 40x oil objective. **B**, average numbers of SIRT-1 foci (red dot) per cell
495 when cells were cultured at different concentrations of D-glucose.

496

497 Figure-7. H₂O₂ mediates high glucose down regulation of SIRT1 to epigenetically
498 activate expression of KSHV lytic gene RTA. **A** and **B**, Western blot detection of SIRT1
499 protein in BCBL1-BAC36 cells that were cultured in RPMI 1640 medium containing
500 10% FBS and 1, 3, or 6 g/L D-glucose (D-Glu) for 24 h, in the absence (**A**) or presence
501 (**B**) of various doses of catalase (Cat). **C**, Western blot detection of SIRT1 protein in
502 BCBL1-BAC36 cells treated with different doses of H₂O₂ and catalase (Cat). **D**, Western

503 blot detection of acetylated histone-3 (H3K9-Ac) and histone-4 (H4K12-Ac), total
504 histone-3 (H3) and histone-4 (H4), RTA and β -tubulin in BCBL1-BAC36 cells that were
505 cultured in RPMI 1640 medium containing 10% FBS and 1, 3, or 6 g/L D-glucose (D-
506 Glu) in the presence or absence of 400 U/ml catalase (Cat) for 24 h. **E** and **F**, ChIP assay
507 detection of acetylated histones (H3K9-Ac and H4K12-Ac) and RNA polymerase II (RN
508 Pol) in RTA promoter in BCBL1-BAC36 cells that were cultured with different
509 concentrations of D-glucose (D-Glu) with and without 400 U/ml catalase (Cat) for 24 h.
510 The relative amount of DNA in RTA promoter (RTA) from each ChIP reaction was
511 determined by qPCR and calculated as the average ratio between the level of ChIP
512 product and that of the input DNA from three repeats (**F**). Real-time PCR products from
513 inputs and ChIP assays were also analyzed in a 1.5% agarose gel (**E**). Differences in the
514 levels of H3K9-Ac, H4K12-Ac, and RN Pol in RTA promoter between cells cultured in
515 medium containing 1 g/L and 3 or 6 g/L D-glucose, or between cells cultured with and
516 without catalase, were all significant with P values <0.005.

517

518

519 REFERENCES

- 520 1. **Chang, Y., E. Cesarman, M. S. Pessin, F. Lee, J. Culpepper, D. M. Knowles,**
521 **and P. S. Moore.** 1994. Identification of herpesvirus-like DNA sequences in AIDS-
522 associated Kaposi's sarcoma. *Science* **266**:1865-1869.
- 523 2. **Broccolo, F., C. Tassan Din, M. G. Vigano, T. Rutigliano, S. Esposito, P. Lusso,**
524 **G. Tambussi, and M. S. Malnati.** 2016. HHV-8 DNA replication correlates with

- 525 the clinical status in AIDS-related Kaposi's sarcoma. *Journal of clinical virology* :
526 the official publication of the Pan American Society for Clinical Virology **78**:47-52.
- 527 3. **Dagna, L., F. Broccolo, C. T. Paties, M. Ferrarini, L. Sarmati, L. Praderio, M.**
528 **G. Sabbadini, P. Lusso, and M. S. Malnati.** 2005. A relapsing inflammatory
529 syndrome and active human herpesvirus 8 infection. *The New England Journal of*
530 *Medicine* **353**:156-163.
- 531 4. **Ensoli, B., M. Sturzl, and P. Monini.** 2001. Reactivation and role of HHV-8 in
532 Kaposi's sarcoma initiation. *Advances in Cancer Research* **81**:161-200.
- 533 5. **Martinelli, C., M. Zazzi, S. Ambu, D. Bartolozzi, P. Corsi, and F. Leoncini.**
534 1998. Complete regression of AIDS-related Kaposi's sarcoma-associated human
535 herpesvirus-8 during therapy with indinavir. *AIDS* **12**:1717-1719.
- 536 6. **Wit, F. W., C. J. Sol, N. Renwick, M. T. Roos, S. T. Pals, R. van Leeuwen, J.**
537 **Goudsmit, and P. Reiss.** 1998. Regression of AIDS-related Kaposi's sarcoma
538 associated with clearance of human herpesvirus-8 from peripheral blood
539 mononuclear cells following initiation of antiretroviral therapy. *AIDS* **12**:218-219.
- 540 7. **Boshoff, C., and R. A. Weiss.** 2001. Epidemiology and pathogenesis of Kaposi's
541 sarcoma-associated herpesvirus. *Philosophical transactions of the Royal Society of*
542 *London. Series B, Biological Sciences* **356**:517-534.
- 543 8. **Ciment, L. M., A. Rotbart, A. Blaustein, R. N. Galbut, and D. Grieder.** 1983.
544 Asthma, Kaposi's sarcoma, and nodular pulmonary infiltrates. *Chest* **84**:281-282.
- 545 9. **Goedert, J. J., F. Vitale, C. Lauria, D. Serraino, M. Tamburini, M. Montella,**
546 **A. Messina, E. E. Brown, G. Rezza, L. Gafa, and N. Romano.** 2002. Risk factors

- 547 for classical Kaposi's sarcoma. *Journal of the National Cancer Institute* **94**:1712-
548 1718.
- 549 10. **Caprio, B., B. Volpini, L. Centi, D. Marri, A. Benvenuti, and E. Falco.** 1985.
550 [Kaposi's sarcoma: on its frequent association with lymphoreticular neoplasms and
551 diabetes mellitus]. *Minerva Medica* **76**:1227-1232.
- 552 11. **Laor, Y., and R. A. Schwartz.** 1979. Epidemiologic aspects of american Kaposi's
553 sarcoma. *Journal of Surgical Oncology* **12**:299-303.
- 554 12. **Ronchese, F., and A. B. Kern.** 1953. Kaposi's sarcoma and diabetes mellitus.
555 *A.M.A. Archives of Dermatology and Syphilology* **67**:95-96.
- 556 13. **Weissmann, A., S. Linn, S. Weltfriend, and R. Friedman-Birnbaum.** 2000.
557 Epidemiological study of classic Kaposi's sarcoma: a retrospective review of 125
558 cases from Northern Israel. *Journal of the European Academy of Dermatology and*
559 *Venereology* **14**:91-95.
- 560 14. **Caselli, E., R. Rizzo, A. Ingianni, P. Contini, R. Pompei, and D. Di Luca.** 2014.
561 High prevalence of HHV8 infection and specific killer cell immunoglobulin-like
562 receptors allotypes in Sardinian patients with type 2 diabetes mellitus. *Journal of*
563 *Medical Virology* **86**: 1745-1751.
- 564 15. **Sobngwi, E, S.P. Choukem, F. Agbalika, B. Blondeau, L.S. Fetita, C. Lebbe, D.**
565 **Thiam, P. Cattan, J. Larghero, F. Fougelle, P. Ferre, P. Vexiau, F. Calvo, and**
566 **J.F.** 2008. Ketosis-prone type 2 diabetes mellitus and human herpesvirus 8
567 infection in sub-saharan africans. *Journal of American Medical Association* **299**:
568 2770-2776.

- 569 16. **Anderson LA, Lauria C, Romano N, Brown EE, Whitby D, B.I. Graubard, Y.**
570 **Li, A. Messina, L. Gafa, F. Vitale, and J.J. Goedert.** 2008. Risk factors for
571 classical Kaposi sarcoma in a population-based case-control study in Sicily. *Cancer*
572 *Epidemiol Biomarkers Prev* **17**: 3435-3443.
- 573 17. **Tokunaga, H., Y. Yoneda, and K. Kuriyama.** 1983. Streptozotocin-induced
574 elevation of pancreatic taurine content and suppressive effect of taurine on insulin
575 secretion. *European Journal of Pharmacology* **87**:237-243.
- 576 18. **An, F. Q., H. M. Folarin, N. Compitello, J. Roth, S. L. Gerson, K. R. McCrae,**
577 **F. D. Fakhari, D. P. Dittmer, and R. Renne.** 2006. Long-term-infected
578 telomerase-immortalized endothelial cells: a model for Kaposi's sarcoma-associated
579 herpesvirus latency in vitro and in vivo. *Journal of Virology* **80**:4833-4846.
- 580 19. **Brulois, K. F., H. Chang, A. S. Lee, A. Ensser, L. Y. Wong, Z. Toth, S. H. Lee,**
581 **H. R. Lee, J. Myoung, D. Ganem, T. K. Oh, J. F. Kim, S. J. Gao, and J. U.**
582 **Jung.** 2012. Construction and manipulation of a new Kaposi's sarcoma-associated
583 herpesvirus bacterial artificial chromosome clone. *Journal of Virology* **86**:9708-
584 9720.
- 585 20. **Li, X., J. Feng, and R. Sun.** 2011. Oxidative stress induces reactivation of Kaposi's
586 sarcoma-associated herpesvirus and death of primary effusion lymphoma cells.
587 *Journal of Virology* **85**:715-724.
- 588 21. **Ye, F., F. Zhou, R. G. Bedolla, T. Jones, X. Lei, T. Kang, M. Guadalupe, and S.**
589 **J. Gao.** 2011. Reactive oxygen species hydrogen peroxide mediates Kaposi's
590 sarcoma-associated herpesvirus reactivation from latency. *PLoS Pathogens*
591 **7**:e1002054.

- 592 22. **Guarente, L.** 2000. Sir2 links chromatin silencing, metabolism, and aging. *Genes*
593 & *Development* **14**:1021-1026.
- 594 23. **Yoo, S. M., F. C. Zhou, F. C. Ye, H. Y. Pan, and S. J. Gao.** 2005. Early and
595 sustained expression of latent and host modulating genes in coordinated
596 transcriptional program of KSHV productive primary infection of human primary
597 endothelial cells. *Virology* **343**:47-64.
- 598 24. **Zhou, F. C., Y. J. Zhang, J. H. Deng, X. P. Wang, H. Y. Pan, E. Hettler, and S.**
599 **J. Gao.** 2002. Efficient infection by a recombinant Kaposi's sarcoma-associated
600 herpesvirus cloned in a bacterial artificial chromosome: application for genetic
601 analysis. *Journal of Virology* **76**:6185-6196.
- 602 25. **Kim, C. H., N. D. Vaziri, and B. Rodriguez-Iturbe.** 2007. Integrin expression and
603 H₂O₂ production in circulating and splenic leukocytes of obese rats. *Obesity*
604 (Silver Spring) **15**:2209-2216.
- 605 26. **Manea, A., E. Constantinescu, D. Popov, and M. Raicu.** 2004. Changes in
606 oxidative balance in rat pericytes exposed to diabetic conditions. *Journal of Cellular*
607 *and Molecular Medicine* **8**:117-126.
- 608 27. **Patel, H., J. Chen, K. C. Das, and M. Kavdia.** 2013. Hyperglycemia induces
609 differential change in oxidative stress at gene expression and functional levels in
610 HUVEC and HMVEC. *Cardiovascular Diabetology* **12**:142.
- 611 28. **Patinha, D., J. Afonso, T. Sousa, M. Morato, and A. Albino-Teixeira.** 2014.
612 Diabetes-induced increase of renal medullary hydrogen peroxide and urinary
613 angiotensinogen is similar in normotensive and hypertensive rats. *Life Sciences*
614 **108**:71-79.

- 615 29. **Watanabe, A., Y. Tomino, K. Yokoyama, and H. Koide.** 1993. Production of
616 hydrogen peroxide by neutrophilic polymorphonuclear leukocytes in patients with
617 diabetic nephropathy. *Journal of Clinical Laboratory Analysis* **7**:209-213.
- 618 30. **Zhang, H., E. Agardh, and C. D. Agardh.** 1991. Hydrogen peroxide production in
619 ischaemic retina: influence of hyperglycaemia and postischaemic oxygen tension.
620 *Diabetes Res* **16**:29-35.
- 621 31. **Ye, F., and S. J. Gao.** 2011. A novel role of hydrogen peroxide in Kaposi sarcoma-
622 associated herpesvirus reactivation. *Cell Cycle* **10**:3237-3238.
- 623 32. **Hernandez-Barrera, A., C. Quinto, E. A. Johnson, H. M. Wu, A. Y. Cheung,**
624 **and L. Cardenas.** 2013. Using hyper as a molecular probe to visualize hydrogen
625 peroxide in living plant cells: a method with virtually unlimited potential in plant
626 biology. *Methods in Enzymology* **527**:275-290.
- 627 33. **Cao, Y., X. Jiang, H. Ma, Y. Wang, P. Xue, and Y. Liu.** 2016. SIRT1 and insulin
628 resistance. *Journal of Diabetes and its Complications* **30**:178-183.
- 629 34. **Cote, C. D., B. A. Rasmussen, F. A. Duca, M. Zadeh-Tahmasebi, J. A. Baur, M.**
630 **Daljeet, D. M. Breen, B. M. Filippi, and T. K. Lam.** 2015. Resveratrol activates
631 duodenal Sirt1 to reverse insulin resistance in rats through a neuronal network.
632 *Nature Medicine* **21**:498-505.
- 633 35. **Guclu, A., F. M. Erdur, and K. Turkmen.** 2016. The Emerging Role of Sirtuin 1
634 in Cellular Metabolism, Diabetes Mellitus, Diabetic Kidney Disease and
635 Hypertension. *Experimental and clinical endocrinology & diabetes : Official*
636 *Journal, German Society of Endocrinology [and] German Diabetes Association*
637 **124**:131-139.

- 638 36. **Jukarainen, S., S. Heinonen, J. T. Ramo, R. Rinnankoski-Tuikka, E. Rappou,**
639 **M. Tummers, M. Muniandy, A. Hakkarainen, J. Lundbom, N. Lundbom, J.**
640 **Kaprio, A. Rissanen, E. Pirinen, and K. H. Pietilainen.** 2016. Obesity Is
641 Associated With Low NAD(+)/SIRT Pathway Expression in Adipose Tissue of
642 BMI-Discordant Monozygotic Twins. *The Journal of Clinical Endocrinology and*
643 *Metabolism* **101**:275-283.
- 644 37. **Kraus, D., Q. Yang, D. Kong, A. S. Banks, L. Zhang, J. T. Rodgers, E. Pirinen,**
645 **T. C. Pulinilkunnil, F. Gong, Y. C. Wang, Y. Cen, A. A. Sauve, J. M. Asara, O.**
646 **D. Peroni, B. P. Monia, S. Bhanot, L. Alhonen, P. Puigserver, and B. B. Kahn.**
647 2014. Nicotinamide N-methyltransferase knockdown protects against diet-induced
648 obesity. *Nature* **508**:258-262.
- 649 38. **Rodgers, J. T., C. Lerin, W. Haas, S. P. Gygi, B. M. Spiegelman, and P.**
650 **Puigserver.** 2005. Nutrient control of glucose homeostasis through a complex of
651 PGC-1alpha and SIRT1. *Nature* **434**:113-118.
- 652 39. **Sheline, C. T.** 2012. Involvement of SIRT1 in Zn, Streptozotocin, Non-Obese
653 Diabetic, and Cytokine-Mediated Toxicities of beta-cells. *Journal of Diabetes &*
654 *Metabolism* **3**: 193. doi:10.4172/2155-6156.1000193.
- 655 40. **He, M., and S. J. Gao.** 2014. A novel role of SIRT1 in gammaherpesvirus latency
656 and replication. *Cell Cycle* **13**:3328-3330.
- 657 41. **Li, Q., M. He, F. Zhou, F. Ye, and S. J. Gao.** 2014. Activation of Kaposi's
658 sarcoma-associated herpesvirus (KSHV) by inhibitors of class III histone
659 deacetylases: identification of sirtuin 1 as a regulator of the KSHV life cycle.
660 *Journal of Virology* **88**:6355-6367.

- 661 42. **Yu, X., A. M. Shahir, J. Sha, Z. Feng, B. Eapen, S. Nithianantham, B. Das, J.**
662 **Karn, A. Weinberg, N. F. Bissada, and F. Ye.** 2014. Short-chain fatty acids from
663 periodontal pathogens suppress histone deacetylases, EZH2, and SUV39H1 to
664 promote Kaposi's sarcoma-associated herpesvirus replication. *Journal of Virology*
665 **88**:4466-4479.
- 666 43. **Bottero, V., S. Chakraborty, and B. Chandran.** 2013. Reactive oxygen species
667 are induced by Kaposi's sarcoma-associated herpesvirus early during primary
668 infection of endothelial cells to promote virus entry. *Journal of Virology* **87**:1733-
669 1749.
- 670 44. **Dai, L., M. R. DeFee, Y. Cao, J. Wen, X. Wen, M. C. Noverr, and Z. Qin.** 2014.
671 Lipoteichoic acid (LTA) and lipopolysaccharides (LPS) from periodontal
672 pathogenic bacteria facilitate oncogenic herpesvirus infection within primary oral
673 cells. *PloS One* **9**:e101326.
- 674 45. **Gjyshi, O., V. Bottero, M. V. Veettil, S. Dutta, V. V. Singh, L. Chikoti, and B.**
675 **Chandran.** 2014. Kaposi's sarcoma-associated herpesvirus induces Nrf2 during de
676 novo infection of endothelial cells to create a microenvironment conducive to
677 infection. *PLoS Pathogens* **10**:e1004460.
- 678 46. **Bordone, L., and L. Guarente.** 2005. Calorie restriction, SIRT1 and metabolism:
679 understanding longevity. *Nature Reviews Molecular Cell Biology* **6**:298-305.
- 680 47. **Csiszar, A., N. Labinskyy, R. Jimenez, J. T. Pinto, P. Ballabh, G. Losonczy, K.**
681 **J. Pearson, R. de Cabo, and Z. Ungvari.** 2009. Anti-oxidative and anti-
682 inflammatory vasoprotective effects of caloric restriction in aging: role of

- 683 circulating factors and SIRT1. *Mechanisms of Ageing and Development* **130**:518-
684 527.
- 685 48. **Yang, J., N. Wang, Y. Zhu, and P. Feng.** 2011. Roles of SIRT1 in high glucose-
686 induced endothelial impairment: association with diabetic atherosclerosis. *Archives*
687 *of Medical Research* **42**:354-360.
- 688 49. **Li, Q., M. He, F. Zhou, F. Ye, and S. J. Gao.** 2014. Activation of Kaposi's
689 sarcoma-associated herpesvirus by inhibitors of class III histone deacetylases:
690 identification of SIRT1 as a regulator of KSHV life cycle. *Journal of Virology* **88**:
691 6355-6367.
- 692 50. **Neugebauer, R. C., W. Sippl, and M. Jung.** 2008. Inhibitors of NAD⁺ dependent
693 histone deacetylases (sirtuins). *Current Pharmaceutical Design* **14**:562-573.
- 694 51. **Vaquero, A., R. Sternglanz, and D. Reinberg.** 2007. NAD⁺-dependent
695 deacetylation of H4 lysine 16 by class III HDACs. *Oncogene* **26**:5505-5520.
- 696 52. **Vaziri, H., S. K. Dessain, E. Ng Eaton, S. I. Imai, R. A. Frye, T. K. Pandita, L.**
697 **Guarente, and R. A. Weinberg.** 2001. hSIR2(SIRT1) functions as an NAD-
698 dependent p53 deacetylase. *Cell* **107**:149-159.
- 699 53. **Greene, W., K. Kuhne., F.C. Ye., J.G. Chen., F.C. Zhou., X.F. Lei., and S.J.**
700 **Gao.** 2007. Molecular biology of KSHV in relation to AIDS-associated
701 oncogenesis. *Cancer Treatment and Research* **133**:69-127.
- 702 54. **Ye, F.C., X.F. Lei., and S.J. Gao.** 2011. Mechanisms of Kaposi's sarcoma-
703 associated herpesvirus latency and reactivation. *Advances in Virology*
704 **2011**:193860.

- 705 55. **Zhu, Y., S. Ramos, Q.M. Liang, C. Lu, P.H. Feng, J.U. Jung, and S. J. Gao.**
706 2016. Suppression of glycolysis by KSHV promotes cell survival and oncogenic
707 transformation. *PLoS Pathogens* **12**:e1005648
708
709
710
711

